Engineering
in Life Sciences

TECHNICAL REPORT

R-based method for quantitative analysis of biofilm thickness by using confocal laser scanning microscopy

Hanna Marianne Frühauf[1,2] | **Markus Stöckl[1]** | **Dirk Holtmann[2]**

[1]Department of Chemical Technology, DECHEMA Forschungsinstitut, Frankfurt am Main, Germany

[2]Institut für Bioverfahrenstechnik und Pharmazeutische Technologie, Technische Hochschule Mittelhessen, Gießen, Germany

Correspondence
Dirk Holtmann, Technische Hochschule Mittelhessen, Wiesenstrasse 14, 35390 Gießen, Germany.
Email: dirk.holtmann@lse.thm.de

Abstract

Microscopy is mostly the method of choice to analyse biofilms. Due to the high local heterogeneity of biofilms, single and punctual analyses only give an incomplete insight into the local distribution of biofilms. In order to retrieve statistically significant results a quantitative method for biofilm thickness measurements was developed based on confocal laser scanning microscopy and the programming language R. The R-script allows the analysis of large image volumes with little hands-on work and outputs statistical information on homogeneity of surface coverage and overall biofilm thickness. The applicability of the script was shown in microbial fuel cell experiments. It was found that *Geobacter sulfurreducens* responds differently to poised anodes of different material so that the optimum potential for MFC on poised ITO anodes had to be identified with respect to maximum current density, biofilm thickness and MFC start-up time. Thereby, a positive correlation between current density and biofilm thickness was found, but with no direct link to the applied potential. The optimum potential turned out to be +0.1 V versus SHE. The script proved to be a valuable stand-alone tool to quantify biofilm thickness in a statistically valid manner, which is required in many studies.

KEYWORDS
biofilm thickness, *Geobacter sulfurreducens*, microbial fuel cells, quantitative method, R-script

1 | INTRODUCTION

Biofilms appear ubiquitously in non-natural habitats like heat exchangers, pipes, hoses, medical implants and catheters but are also applied in catalytic processes. Heterogeneity in biofilm growth plays an important role in controlling biofouling, biocorrosion or application of antibiotics as well as improving production processes with catalytic biofilms. From an engineering point of view, one of the first steps required is to assess the statistical significance (or possibly insignificance) of heterogeneity in biofilm growth and its variability [3].

Confocal laser scanning microscopy (CLSM) is a non-destructive and non-invasive method with the capability to provide three-dimensional images of biofilms. The analysis of the obtained CLSM data is very often rather qualitative than quantitative and based on a subjective visual image inspection. This approach is however not feasible when large quantities of data have to be analysed, which

Abbreviations: CLSM, confocal laser scanning microscopy; ITO, indium-tin oxide; MFC, microbial fuel cells

is often necessary to ensure the significance of the outcome of the CLSM measurements [4]. In order to perform a quantitative analysis an R-based method was developed and evaluated in a bioelectrochemical process with the biofilm-forming and electroactive organism *Geobacter sulfurreducens*.

G. sulfurreducens is a model organism in microbial fuel cell (MFC) research and known for its good ability to form biofilms on the electrode and high current densities produced from complete acetate oxidation [5]. Mostly, carbon-based materials are used as anode material because of their good biocompatibility, corrosion-resistance and cost-effectiveness [6]. Especially for spectroscopic methods in connection with biofilm analysis transparent anodes are required like indium-tin oxide (ITO) or gold sputtered glass slides (e.g. in [7–9]). Most lab-scale MFC are operated with poised anodes to drive *G. sulfurreducens* extracellular electron transfer. Thereby, the more positive the potential, the higher the energy supplied to the system. Direct electron transfer between *G. sulfurreducens* and the anode is based on a relay of outer membrane cytochromes (Omc) and conductive pili [10–13]. This network allows the formation of conductive biofilms in which also the outer cell layers are electrically "wired" to the anode [14–16]. It was shown that the applied potential influences the type of Omc active in electron transport as well as the composition of the extracellular polymeric substances present in the biofilm [17–19]. What has been little discussed so far is the interpolated effect of electrode material and applied potential. *G. sulfurreducens* MFC were conducted at different potentials on ITO electrodes to determine a potential which optimises the MFC performance indicators maximum current density, start-up phase and biofilm thickness. The latter characteristic is often only evaluated qualitatively when CLSM is used for analysis as manual thickness determination from CLSM images is laborious and time-consuming. CLSM is the method of choice as it allows rapid qualitative evaluation of biofilm heterogeneity, electrode coverage and cell viability (if appropriate staining methods are used). With fluorescent strains biofilms can also be analysed in vivo, that is, during the experiment, which gives insights into MFC start-up time for example. Other methods for thickness determination require the knowledge of the biofilm refractive index (analysis with light microscopy) [20], additional preparatory steps like cryo-cut [3] or special equipment, unusual in bioelectrochemical applications (low-load compression testing in [21]).

The optimisation of *G. sulfurreducens* MFC performance on ITO electrodes was used as a proof-of-principle for a quantitative method that measures biofilm thickness based on CLSM imaging of fluorescently stained biofilms

PRACTICAL APPLICATION

Biofilm communities can be found in every habitat in which water, nutrients and a colonisable surface are present. Depending on the surface, biofilms can cause economic losses due to bio-corrosion or can be a severe threat to human health [1–2]. Desirable are catalytic biofilms for example in bioelectrochemical production processes. In all cases, quantitative and qualitative biofilm analysis is necessary in order to help to prevent or promote biofilm formation and to link productivity with biomass deposited on the electrode. CLSM analysis allows the recording of high volumes of image data but often image analysis then remains at a qualitative stage, for example estimating biofilm thickness from a small amount of images. The presented R-script allows the calculation of biofilm thickness based on large data sets and allows conclusions on the homogeneity of biofilm surface coverage. The script is a stand-alone tool if only biofilm thickness should be determined and does not require any image segmentation or processing.

and statistical evaluation with the programming language R [22]. It is a stand-alone method that does not require image segmentation or filtering and allows statistical analysis of a high volume of biofilm images with little hands-on work. Explanation and evaluation of the R-script is central to this publication, and the optimisation of MFC performance on ITO electrodes should be seen as an exemplary application rather than a profound explanation of the biological phenomenon.

2 | MATERIALS AND METHODS

2.1 | Cultivation of *G. sulfurreducens*

G. sulfurreducens strain PCA (DSM 12127) was obtained from DSMZ (German collection of Microorganisms and Cell Cultures GmbH, Braunschweig, Germany). All cultivations were done anaerobically in serum flasks sealed with a butyl septum. Flasks were incubated shaking at 30°C and 180 rpm. Growth medium was DSM826 as recommended by DSMZ, but with 30 mM Na_2-fumarate instead of 50 mM as soluble electron acceptor. Cultivation conditions were also described in Ref. [23].

2.2 | Microbial fuel cell experiments with *G. sulfurreducens*

MFC experiments were carried out in a modified electrochemical H-cell, as described in Ref. [23]. In this setup the WE is flanged to the WE chamber from one side which ensures a stable fixation in the reactor and thereby stable flow conditions for bacterial adhesion and biofilm growth. ITO coated glass was used as WE (30 mm × 30 mm × 1.1 mm; resistance 20 Ω cm^{-2}; Präzisions Glas & Optik GmbH, Iserlohn, Germany) with graphite paper for contacting (0.13 mm thin, type RCT$^{®}$-DKA-SBGR; RCT Reichelt Chemietechnik GmbH + Co., Heidelberg, Germany) and graphite as counter electrode (Bipolar plate, Eisenhuth GmbH & Co. KG, Osterode am Harz, Germany). Experiments were conducted at constant potential by using IPS (Elektronik GmbH & Co KG, Münster, Germany) and Gamry potentiostats (Reference600 and Interface1000; Gamry Instruments, Warminster, PA) with Ag/AgCl/KCl$_{sat}$ reference electrode (E = + 0.19 V vs. SHE; Sensortechnik Meinsberg, Waldheim, Germany) that was placed in a Haber-Luggin-capillary filled with KCl$_{sat}$. Both chambers were filled with growth medium lacking the soluble electron acceptor fumarate.

2.3 | CLSM analysis

Immediately after an experiment was aborted, biofilms were stained with the fluorescent dyes SYTO^{TM}9 Green Fluorescent Nucleic Acid Stain (Syto9) and Propidium iodide (PI; both Invitrogen^{TM}, Waltham MA, USA). Stock solutions in 0.125 M phosphate buffer were 6 mM Syto9 and 30 mM PI. Dyes were mixed 1:1 in a final volume of 400 μL per biofilm (stained area 5 cm^2). Electrodes with biofilms were carefully detached from the WE chamber, placed in a petri dish (5 cm diameter), overlaid with 400 μL staining solution and incubated for 15 min in the dark. Afterwards, staining solution was removed and the biofilm rinsed three times with 0.125 M phosphate buffer, the fourth buffer volume remained on the biofilm to avoid desiccation.

Microscopic images were acquired with a TCS SP8 CLSM (Leica Microsystems GmbH, Wetzlar, Germany) with galvanometric stage. In order to image the biofilm in a hydrated state and thereby retrieving a realistic value for biofilm thickness, a dip-in objective was used (HC APO UVIS CS2, 63× magnification, numerical aperture 0.9, refraction index 1.33) that allowed imaging while the biofilms were stored in a petri dish, filled with buffer. Laser intensity (OPSL 488) was set to 5% and an excitation beam splitter DD488/552 used with the PMT detector set to emission wavelengths between 500 and 545 nm (for the green
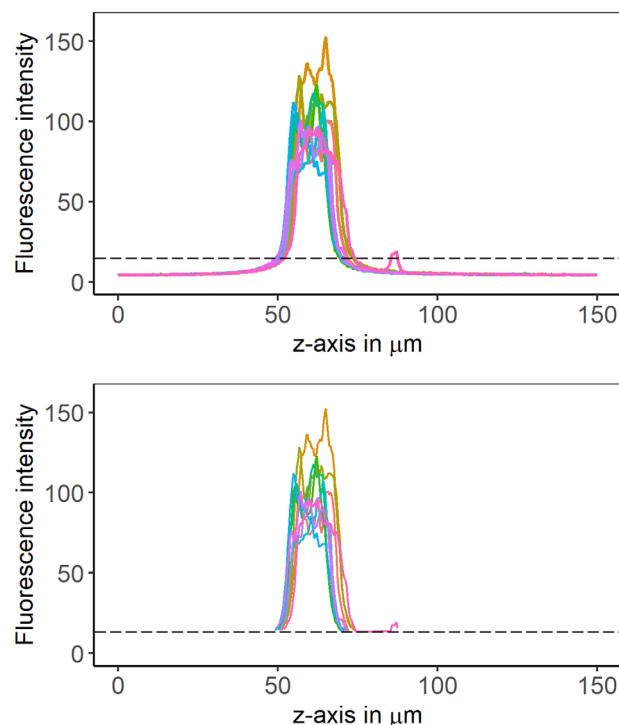

FIGURE 1 Fluorescence intensity of 10 ROI in one z-image are plotted against the z-dimension, before (top) and after (bottom) background subtraction. The dashed line indicates the threshold cut off. The area to the right of the maximum is biologically above the biofilm, that is, buffer and planctonic cells. To the left is the electrode accordingly. In the shown example a fluorescence signal caused by planctonic cells could not be subtracted by the defined threshold, hence additional data treatment was needed so that biofilm thickness is not overestimated

channel) and the HyD between 615 and 788 nm (for the red channel). The basis to determine biofilm thickness was z-images of a 185 μm wide area taken on ten randomly chosen sections on the biofilm. For optimum analysis laser intensity should be chosen in a way that the biofilm is clearly distinguished but not overexposed. The Syto9 fluorescence signal was subsequently used as input for quantitative analysis of biofilm thickness and the combination of Syto9 and PI (also known as live/dead staining) to qualitatively assess biofilm viability.

2.4 | Quantification of biofilm thickness using R

Ten regions of interest (ROI) were defined on the z-images, each with one tenth of the image width, that is, 18.5 μm (shown in Figure S1). Fluorescence intensity wa s recorded along the length of each ROI and plotted against the z-axis, resulting in a histogram (Figure 1). The thickness of

the biofilm was extracted from the range of the histogram in which fluorescence was above a certain threshold level that defined the background fluorescence (indicated by the dashed line in Figure 1). Histogram data were exported from the LAS X software (Version 3.5.5) as .csv files which were then input for the R-script with which biofilm thickness was calculated.

The R-script is shown in the SI and provided as .txt file along with this paper. The basic function of the script is explained in the following, with further details in the SI. The R-packages needed are data.table, reshape2, dplyr, (ggplot2 and cowplot for plotting). The .csv-files exported from LAS X must be converted to UTF-8 first, otherwise the R function *fread* is unable to read the files. This can be done for example with the online tool subtitletools, available at https://subtitletools.com/convert-text-files-to-utf8-online. The fluorescence intensity data (line profiles) that were used in this study are available in "figshare" at https://doi.org/10.6084/m9.figshare.19165097.v1.

Pixels in the z-image that belong to the biofilm (and not to the background) are defined as those with intensity higher than three-times the mean intensity of the background signal. All background pixels are replaced with NA, which is an "empty" value for the script. Since the background above the biofilm (buffer and planctonic cells) and below (electrode) have different background intensities the calculation is performed separately for left (first line; id < id_max) and right (first line; id > id_max) of the histogram's maximum (script line 36–40). That is why the information about the histogram peak was stored in the data column "id_max" before (line 35). Here, the threshold is defined as three-times mean background intensity but for higher background signal, that is, background fluorescence of a different electrode material the threshold might need to be adapted (e.g. two-times the background signal).

While the border between the electrode and the biofilm is defined as the point at which the intensity exceeds 3*mean(background signal), it is more difficult for the "End" of the biofilm (the transition between the biofilm and the buffer). Even though the biofilm is washed prior to CLSM analysis there are always cells floating above the biofilm that disturb the measurement. These fluorescent spots on the image can have signal intensity > 3-times background intensity and thereby falsify the definition of the biofilm end (see Figure 1). A rescue for this is to define the first occurring case in the histogram at which the intensity is < 3*mean(background) as the biofilm end. Since row numbers were added to the data table in the beginning (line 34) and all background pixels were eliminated from the table afterwards, the first case is the first gap in the consecutive row number column (with id > id_max, i.e. after maximum of the histogram). The gap can be detected by

calculating the difference between entries of the row number column (line 68–73). Hence, the script "searches" for any difference other than 1 (line 74–76). While this solves the problem for the "End" of the biofilm, it might now overlook the "Beginning" of the biofilm if there is no gap in the row number. This is bypassed by doubling the first row of each histogram (line 64–67). The difference in row number is then 0 for these cases and thereby grabbed by the script. When the difference is calculated, the resulting data column is one entry short compared to the row number column, so an additional entry had to be added to the column (0 in this case) (line 70–71).

3 | RESULTS AND DISCUSSION

G. sulfurreducens MFC were performed on ITO electrodes, poised at different potentials (−0.1, 0, +0.05, +0.1, +0.2, +0.3 V vs. SHE) to identify the potential with the best response with respect to the performance parameters maximum current density, start-up phase and biofilm thickness. Results are shown in Table 1 (mean and SD of $n = 3$). Parameters related to current production were extracted from the potentiostat record and biofilm thickness determined with the developed R-script.

In order to assess any interdependence between the applied potential and the MFC performance indicators, Pearson correlation coefficients (r) were calculated, using the function *rcorr()* from the R-package *Hmisc*. Mathematically, there was no linear correlation between the applied potential and any of the performance indicators but biofilm thickness correlated positively the maximum current density ($r = 0.79$, $p < 0.0001$), hence the thicker the biofilm, the higher the maximum current. The correlation is illustrated in Figure 2 which shows the maximum current density of each experiment plotted against the measured biofilm thickness. Noticeable is the high deviation for the triplicates (three experiments with identical
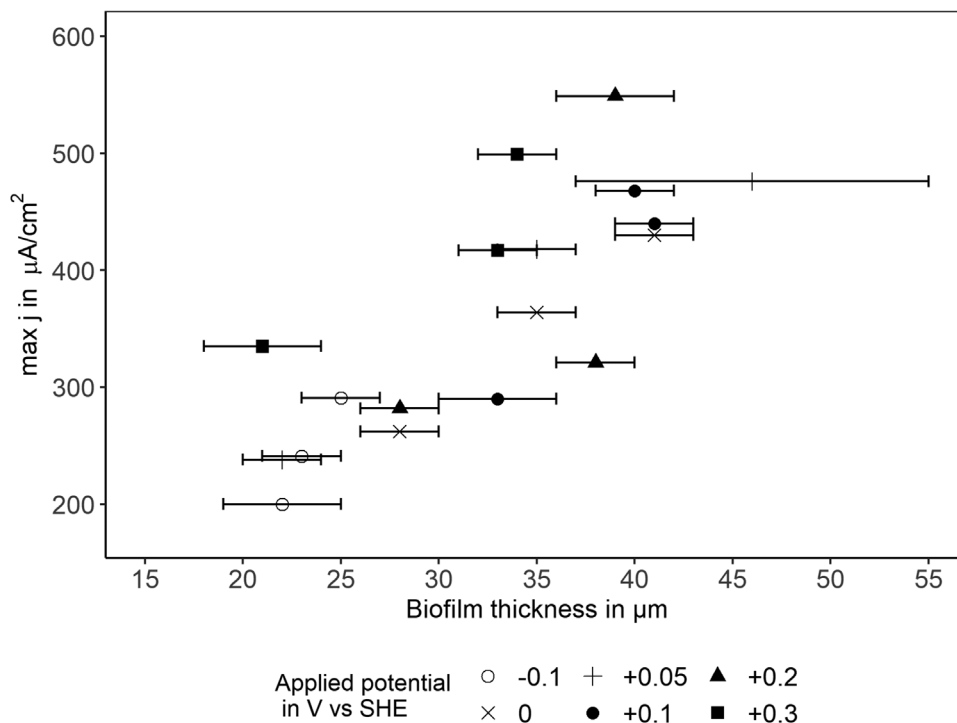
TABLE 1 Maximum current density, start-up time, biofilm thickness and CE for different potentials applied in MFC on ITO electrodes. Indicated are mean values ± SD ($n = 3$)

Applied potential in V vs. SHE	Maximum current density in μA cm^{-2}	Start-up time in h	Biofilm thickness in μm
−0.1	244 ± 19%	20.4 ± 20%	23 ± 7
0	352 ± 24%	19.8 ± 13%	35 ± 6
+0.05	377 ± 35%	20.0 ± 26%	34 ± 13
+0.1	399 ± 24%	19.2 ± 7%	38 ± 7
+0.2	384 ± 38%	22.3 ± 4%	35 ± 7
+0.3	417 ± 20%	41.4 ± 12%	29 ± 7

FIGURE 2 The maximum current density *j* is plotted against the mean biofilm thickness (*n* = 10) to illustrate the positive correlation. Horizontal error bars show SD of ten z-images analysed on each biofilm

potential applied but conducted on different days) in maximum current density, which is the highest for +0.05 and +0.2 V vs. SHE applied (35, respectively 38%). Despite the deviation for the triplicates the positive correlation is still valid if all experiments are treated individually. As biofilm thickness is measured methodically at different areas on the electrode, each thickness measurement for whole electrodes is automatically linked to an estimate of the statistical uncertainty (shown as horizontal error bar in Figure 2). The width of the error bar indicates the homogeneity of thickness on the whole electrode area. The experiment polarised at +0.05 V vs. SHE with the highest maximum current density for example shows a higher SD compared to the other electrodes (±9 μM).

The reason for this can be seen in Figure 3 which displays the determined thickness for the electrode polarised to +0.05 V versus SHE with the highest deviation. Shown are boxplots of ten ROI assigned per image, with the corresponding position on the electrode on the *x*-axis. The thickness for 7, 8, 9 and 10 is significantly larger compared to the other images. The location of the images on the electrode are marked in the image insert and displays that in this experiment the lower part of the electrode was significantly more attractive for biofilm formation compared to the centre or the upper part. To be sure that this was not a methodical error, the results from the script were reviewed with the z-images and a qualitative assessment of the thick-

ness by laying out a scale was done. The results from the script and the manual analysis differed by a mean of 7% (*n* = 10, SD = 2%) which verifies the results from the script as a true biological effect.

4 | CONCLUDING REMARKS

The described method allowed a statistically significant assessment of homogeneity of biofilm coverage on the electrode as well as the identification of a correlation between biofilm thickness and current density that did not depend directly on the applied potential. The most favourable potential on ITO anodes was +0.1 V versus SHE with a maximum current density of almost 400 μA cm^{-2} and 38 ± 7 μm biofilm thickness. Of course, biofilm thickness determination can also be done manually but is less accurate and more time consuming, as well as the variation within one z-image cannot be included. For the script developed in this work no image correction has to be performed which simplifies the analysis additionally. The recently published software package "BiofilmQ" [24] also covers biofilm thickness calculation, among a vast number of other functions but might be oversized for some applications. Further, "BiofilmQ" is based on Matlab, so if there is an existing R routine the stand-alone script from this work could easily be integrated. The presented
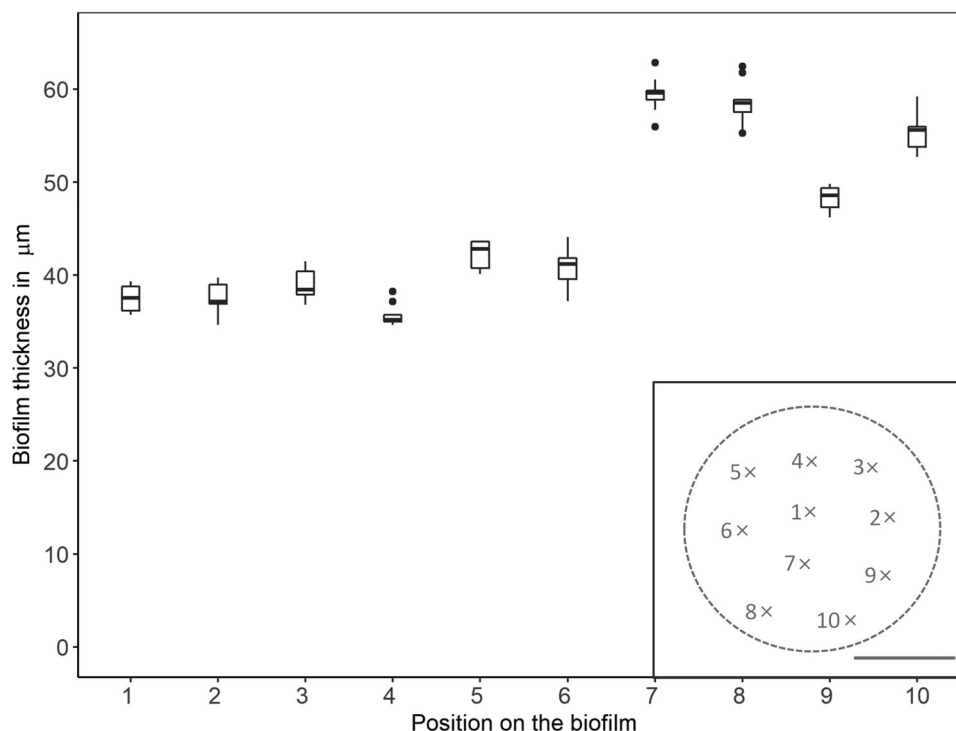
FIGURE 3　Calculated biofilm thickness is plotted with the corresponding location on the biofilm (position on x-axis, approximate position mapped on biofilm in insert). The scale bar in the insert is equivalent to 1 cm

open-access script can be applied to all experimental questions for which analysis of biofilm thickness and finally biofilm topology is scientifically or technically relevant.

CONFLICT OF INTEREST
The authors have declared no conflicts of interest.

DATA AVAILABILITY STATEMENT
The data that support the findings of this study are openly available in "figshare" at https://doi.org/10.6084/m9.figshare.19165097.v1.

REFERENCES
1. Hall-Stoodley L, Costerton JW, Stoodley P. Bacterial biofilms: from the natural environment to infectious diseases. *Nat Rev Microbiol*. 2004;2:95-108.
2. Dou W, Xu D, Gu T. Biocorrosion caused by microbial biofilms is ubiquitous around us. *Microb Biotechnol*. 2021;14:803-805.
3. Murga R, Stewart PS, Daly D. Quantitative analysis of biofilm thickness variability. *Biotechnol Bioeng*. 1995;45:503-510.
4. Heydorn A, Ersbøll BK, Hentzer M, et al. Experimental reproducibility in flow-chamber biofilms. *Microbiology*. 2000;146:2409-2415.
5. Bond DR, Lovley DR. Electricity production by Geobacter sulfurreducens attached to electrodes. *Appl Environ Microbiol*. 2003;69:1548-1555.
6. Baudler A, Schmidt I, Langner M, et al. Does it have to be carbon? Metal anodes in microbial fuel cells and related bioelectrochemical systems. *Energy Environ Sci*. 2015;8:2048-2055.
7. Robuschi L, Tomba JP, Busalmen JP. Proving Geobacter biofilm connectivity with confocal Raman microscopy. *J Electroanal Chem*. 2017;793:99-103.
8. Song F, Koo H, Ren D. Effects of material properties on bacterial adhesion and biofilm formation. *J Dent Res*. 2015;94:1027-1034.
9. Scarabotti F, Rago L, Bühler K, Harnisch F. The electrode potential determines the yield coefficients of early-stage Geobacter sulfurreducens biofilm anodes. *Bioelectrochemistry*. 2021;140:107752.
10. Nevin KP, Richter H, Covalla S, et al. Power output and columbic efficiencies from biofilms of *Geobacter sulfurreducens* comparable to mixed community microbial fuel cells. *Environ Microbiol*. 2008;10:2505-2514.
11. Nevin KP, Kim B-C, Glaven RH, et al. Anode biofilm transcriptomics reveals outer surface components essential for high density current production in *Geobacter sulfurreducens* fuel cells. *PLoS One*. 2009;4:e5628.
12. Mehta T, Coppi MV, Childers SE, Lovley DR. Outer membrane c-type cytochromes required for Fe (III) and Mn (IV) oxide reduction in Geobacter sulfurreducens. *Appl Environ Microbiol*. 2005;71:8634-8641.

13. Bond DR, Strycharz-Glaven SM, Tender LM, Torres CI. On electron transport through Geobacter biofilms. *ChemSusChem.* 2012;5:1099.

14. Reguera G, Nevin KP, Nicoll JS, et al. Biofilm and nanowire production leads to increased current in *Geobacter sulfurreducens* fuel cells. *Appl Environ Microbiol.* 2006;72:7345-7348.

15. Reguera G, McCarthy KD, Mehta T, et al. Extracellular electron transfer via microbial nanowires. *Nature.* 2005;435:1098-1101.

16. Liu X, Walker DJ, Nonnenmann SS, et al. Direct observation of electrically conductive pili emanating from *Geobacter sulfurreducens. Mbio.* 2021;12:e02209-21.

17. Li DB, Li J, Liu DF, et al. Potential regulates metabolism and extracellular respiration of electroactive *Geobacter biofilm. Biotechnol Bioeng.* 2019;116:961-971.

18. Liu D-F, Li W-W, Potential-dependent extracellular electron transfer pathways of exoelectrogens. *Curr Opin Chem Biol.* 2020;59:140-146.

19. Yang G, Huang L, Yu Z, et al. Anode potentials regulate Geobacter biofilms: new insights from the composition and spatial structure of extracellular polymeric substances. *Water Res.* 2019;159:294-301.

20. Bakke R, Olsson P, Biofilm thickness measurements by light microscopy. *J Microbiol Methods.* 1986;5:93-98.

21. Paramonova E, De Jong ED, Krom BP, et al. Low-load compression testing: a novel way of measuring biofilm thickness. *Appl Environ Microbiol.* 2007;73:7023-7028.

22. R Core Team, *R: A Language and Environment for Statistical Computing*, R Foundation for Statistical Computing; 2019.

23. Stöckl M, Teubner NC, Holtmann D, et al. Extracellular polymeric substances from *Geobacter sulfurreducens* biofilms in microbial fuel cells. *ACS Appl Mater Interfaces.* 2019;11:8961-8968.

24. Hartmann R, Jeckel H, Jelli E, et al. Quantitative image analysis of microbial communities with BiofilmQ. *Nat Microbiol.* 2021;6:151-156.

SUPPORTING INFORMATION

Additional supporting information may be found in the online version of the article at the publisher's website.